OPEN ACCESS

PRZEGLĄD ELEKTROTECHNICZNY

Hakam Al ZOUABI[1], Christian KREISCHER[2],
Cezary JEDRYCZKA[3], Lucas STEINACKER[4]
ORCID: [1]0009-0009-0486-8353, [2]0000-0002-3627-1844,
[3]0000-0001-5427-059X, [4]0009-0007-0171-0118

DOI: 10.15199/48.2025.11.7

Development of an analytical calculation model for C-core radial flux switching machines with permanent magnet or electrical excitation

Opracowanie analitycznego modelu obliczeniowego dla maszyn przełączających strumień promieniowy z rdzeniem C i magnesem trwałym lub wzbudzeniem elektrycznym

[1] Hakam Al Zouabi, Helmut Schmidt University: Hamburg, DE
[2] Christian Kreischer, Helmut Schmidt University: Hamburg, DE
[3] Cezary Jedryczka, Poznań University of Technology: Poznań, PL
[4] Lucas Steinacker, Helmut Schmidt University: Hamburg, DE

Correspondence address: alzouabh@hsu-hh.de

Abstract: This paper focuses on the analytical formulation of radial air gap flux density distribution of a flux switching permanent magnet and electrically excited machine with C-core shape. The results are verified by the means of a finite element analysis (FEA).

Keywords: flux switching machines, air gap flux density, carter factor, finite element analysis, high temperature superconductors

Streszczenie: W artykule tym skupiono się na analitycznej metodzie wyznaczenia rozkładu gęstości strumienia magnetycznego w szczelinie powietrznej w maszynie synchronicznej o przełączalnym strumieniu magnetycznym. Rozważono maszynę z rdzeniem w kształcie litery C o wzbudzeniu magnesami trwalymi oraz maszynę wzbudzoną uzwojeniem nadprzewodzącym. Wyniki zweryfikowano na podstawie rozkładów pól wyznaczonych metodą elementów skończonych (MES).

Słowa kluczowe: maszyny o przełączalnym strumieniu, rozklad indukcji w szczelinie powietrznej, współczynnik cartera, analiza mes, nadprzewodniki wysokotemperaturowe

Introduction

The flux switching permanent magnet machine has been gaining increasing interest from researchers lately. The machine has high torque density and efficiency like PMSM (Permanent magnet synchronous machine) and the robust and magnet-free rotor design of a SRM (switched reluctance motor) [1]. The machine consists of a simple rotor that is similar to an SRM and a stator in which both the winding and permanent magnets are mounted (Fig. 1).

This type of machine allows for better cooling of the permanent magnets as they are located in the stator.

This allows the reduction of the overall cost of the machine when magnets of lower operating temperatures -like NdFeB- are used [2]. Reducing the cost of magnets is a critical factor for offshore wind turbine generators, especially since gearless direct drive systems are preferred due to their high reliability requirements. Furthermore, using high temperature superconductors (HTS) excitation winding instead of permanent magnets could also benefit strongly from more robust cooling systems and save tons of permanent magnets greatly reducing the overall weight of the machine. Although finite element analysis (FEA) of the magnetic field distribution provides the most accurate method for evaluating FSPM performance, its use in design and optimization is limited by its high computational demands. To address these limitations,

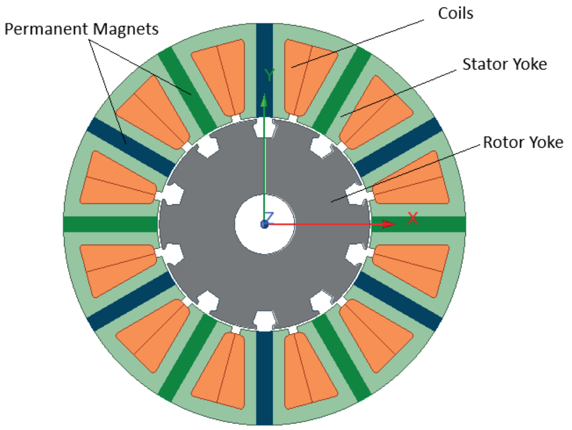

Fig. 1. Cross section of the magnetic circuit of flux switching permanent magnet machine (FSPM)

researchers have developed analytical models [1][3][5] to estimate the performance of FSPM more efficiently. In [1] the authors developed analytical models for both the permanent magnets and the stator coils air gap field density while in [3] a model for DC-field excitation is developed. This work aims to combine both approaches while offering more details regarding the magnetic equivalent circuits. Furthermore, a more detailed consideration of the slotted machine is offered. The future goal of the study is to create an optimizing algorithm based on the analytical model which can achieve designs with the highest torque density and least cogging torque.

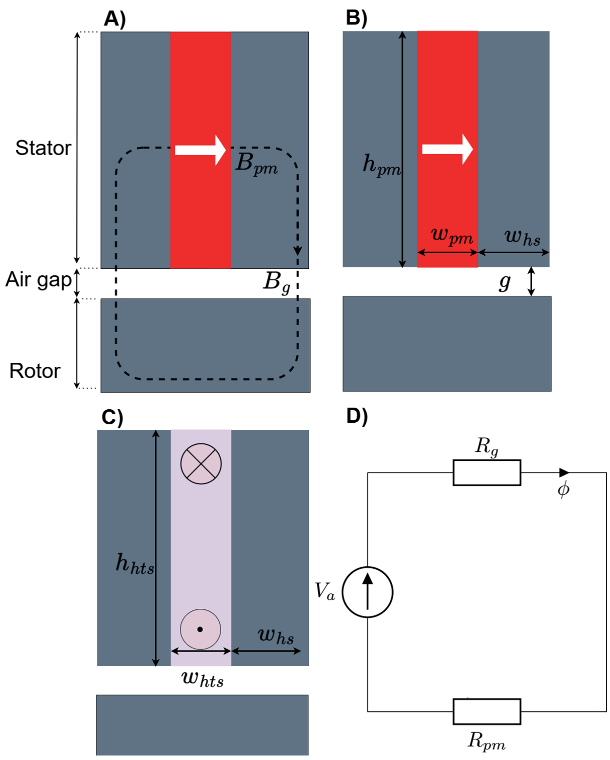

Fig. 2. A) Magnetic flux path, B) Stator tooth geometry, C) Replacing PMs with HTS, D) Magnetic equivalent circuit (MEC) of a permanent magnet

Analytical formulation

Air gap permanent magnet flux density

The radial component of the permanent magnet flux density in the air gap assumes a flux path as given in Fig. (2.A). The geometry of the stator causes a change in the flux cross sectional area, which is simplified to a flux density at the permanent magnet surface B_{pm} and a flux density at the air gap B_g. The permanent magnet flux density could be calculated from a magnetic equivalent circuit (MEC) that assumes a magnetomotive force (MMF) source with two series reluctances representing a voltage drop across the permanent magnet and the air gap as shown in Fig. (2.D). The model assumes no voltage drops across the stator/rotor iron, therefore saturation is neglected.

From the voltage balance of the MEC:

(1) $$V_a = R_{pm}\phi + R_g\phi$$

Which leads to:

(2) $$\frac{B_r w_{pm}}{\mu_m} = \frac{w_{pm}}{A_{pm}\mu_0}\phi + \frac{2g}{A_{hs}\mu_0}\phi$$

With B_r, w_{pm}, μ_m, μ_{pm}, A_{pm}, A_{hs}, g being remanent flux density of PMs, PMs width, permeability of the magnet, permeability of air, surface area of the magnet, surface area of the stator half tooth, and air gap length, respectively.

Using flux conservation between the flux density at the air gap and the magnet surface $\varphi = B_{pm}A_{pm} = B_gA_{hs}$, assuming $\mu_m = \mu_0$ and solving for the flux density in the air gap yields:

(3) $$B_{g,max} = \frac{B_r}{\frac{w_{hs}}{h_{pm}} + \frac{2g}{w_{pm}}}$$

After getting the maximum flux density a trapezoidal wave could be constructed with the following equation using a Fourier series [3]:

(4) $$B_g(\theta) = \sum_{n=1,2,3} b_n \sin\left(\frac{n\theta N_s}{2}\right)$$

Where:
b_n – Amplitude factor of the radial flux density component of each harmonic,
θ – Mechanical angle [rad],
N_s Number of slots.

Equation (4) provides a model of the permanent magnets flux density in the air gap as shown in Fig. (3).

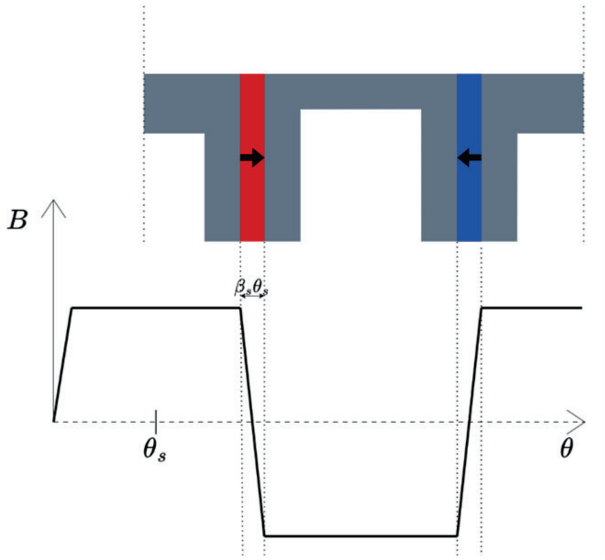

Fig. 3. Permanent magnets flux density in the air gap [3]

The value b_n is determined with the equation:

$$b_n = 2B_{g,max}\left(\frac{8}{\beta_s(n\pi)^2}\right)\sin\left(\frac{n\beta_s\pi}{4}\right) \tag{5}$$

Where β_s is a factor that defines the relationship between the magnet width and the half pole arc.

HTS excitation air gap flux density

To calculate the air gap flux density for an HTS coil with N turns and the current i the same equations could be used but equation (2) needs to be adjusted to:

$$Ni = \frac{w_{hts}}{A_{hts}\mu_0}\phi + \frac{2g}{A_{hs}\mu_0}\phi \tag{6}$$

After following the same derivation, the following equation for the air gap flux density is obtained:

$$B_{hts,max} = \frac{Ni}{\frac{2g}{\mu_0} + \frac{w_{hts}w_{hs}}{h_{hts}\mu_0}} \tag{7}$$

The air gap flux density could be similarly obtained with (4).

Air gap reaction flux density

The stator air gap flux density could also be modelled assuming the flux paths given in Fig. (4). With every flux significantly influencing only the neighbouring slot, further paths of the magnetic flux are neglected. The corresponding MEC is shown in Fig. (5). The circuit includes the reluctance of the permanent magnets (which is treated like air) and the reluctance of the air gap. The source of the magnetic voltage (MMF) is the stator coil current.

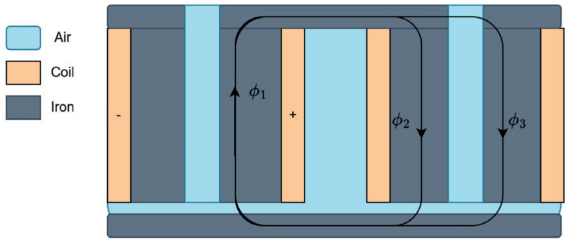

Fig. 4. Magnetic field path in stator due to current

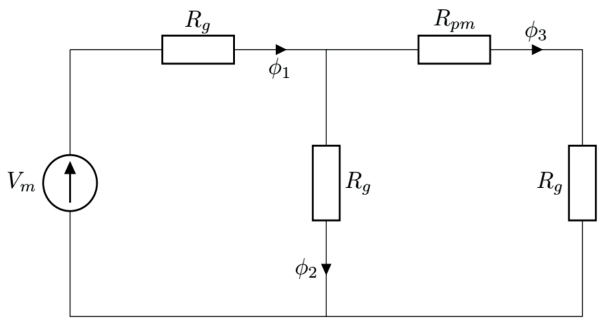

Fig. 5. Magnetic equivalent circuit of half stator coil

The magnetic voltage V_m, the reluctances of the air gap R_g,and permanent magnet R_{pm} are given by:

$$V_m = NI \tag{8}$$

$$R_g = \frac{g}{A_{hs}\mu_0} \tag{9}$$

$$R_{pm} = \frac{w_{pm}}{A_{pm}\mu_0} \tag{10}$$

Solving for the fluxes yields:

$$\phi_1 = \frac{V_m}{\frac{(R_{pm}+R_g)(R_g)}{2R_g+R_{pm}} + R_g} \tag{11}$$

$$\phi_2 = \frac{V_m - R_g\frac{V_m}{\frac{(R_{pm}+R_g)(R_g)}{2R_g+R_{pm}} + R_g}}{R_g} \tag{12}$$

$$\phi_3 = \frac{V_m - R_g\frac{V_m}{\frac{(R_{pm}+R_g)(R_g)}{2R_g+R_{pm}} + R_g}}{R_g + R_{pm}} \tag{13}$$

The flux density is then obtained by dividing the fluxes by the area of a half slot tooth:

$$B_{1,2,3} = \frac{\phi_{1,2,3}}{A_{hs}} \tag{14}$$

The area A_{hs} is calculated as follows:

(15) $$A_{hs} = l_a \frac{\frac{2\pi R_{si}}{N_s} - (R_{si}\frac{\pi}{180}\alpha_s + w_{pm})}{2}$$

With:
α_s – *Stator slot opening [°],*
R_{si} *Stator internal radius [mm],*
N_s *Number of stator slots,*
l_a *Axial length of the machine [mm].*

The previous equations need to be solved for each phase. After that the different fluxes need to be summed up using superposition.

Stator and Rotor Slotting effect

The magnetic flux density near a slot is reduced, this could be understood as an increase of the air gap length.

According to [4] an iterative process could be used to approximate the magnetic flux density. First an equivalent slot opening must be determined, the relation between the geometrical and equivalent slot opening is:

(16) $$b_e = k \cdot b_0$$

The factor k is given with:

(17) $$k = \frac{2}{\pi}\left[\arctan\left(\frac{b_0}{2g}\right) - \frac{2g}{b_0} ln\sqrt{1+\left(\frac{b_0}{2g}\right)^2}\right]$$

The minimum flux density near a slot B_{min} is related to the maximum flux density B_{max} by:

(18) $$B_{min} = B_{max}\frac{2u}{1+u^2}$$

Where:

(19) $$u = \frac{b_0}{2g} + \sqrt{1+\left(\frac{b_0}{2g}\right)^2}$$

The flux density deviation near the slot could be approximated with Carter theory as a step function which has the value of zero in the equivalent slot length and maximum density in the surrounding region [4]. The step function is then replaced by the function $\sin^n(x)$ with the condition that the region $S2$ is equal to $2 \cdot S1$ as shown in Fig. (6).

Estimating the exponent n in the function $f(x) = \sin^n(x)$ requires an iterative process until the condition regarding the areas (S1, S2) is fulfilled. Using this method a corrected magnetic flux is calculated

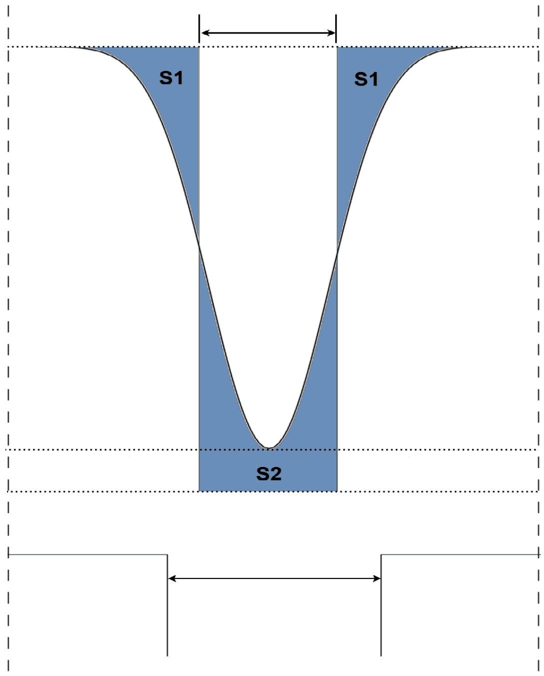

Fig. 6. Variation of magnetic field near a slot [4]

that considers the slotting effect of the rotor, stator and permanent magnets.

After estimating n the flux density considering slotting effect is calculated with:

(20) $$B(\theta) = B_{max} - \left|(B_{max} - B_{min})\sin^n\left(\theta \cdot \frac{N}{2}\right)\right|$$

Where N is the number of rotor or stator slots.
with $B_{max} = 1$the permeance function is calculated as:

(21) $$\lambda(\theta) = 1 - \left|\left(1 - \frac{2u}{1+u^2}\right)\sin^n\left(\theta \cdot \frac{N}{2}\right)\right|$$

Because $\lambda(\theta)$ is only a function of the geometry the slotted flux density could always be calculated with:

(22) $$B_{slotted} = B_{unslotted}\sum_i \lambda_i$$

Where i is the number of considered permeance functions.

FEM Simulation

In the following section a 2D FEM simulation is presented for a 3 phase 48 slots/56 poles machine configuration based on [2]. The full geometry of the machine is illustrated in Fig. (7). A 45° sector is shown in Fig. (8). While geometrical and electrical aspects are explained in Table 1. Two variants of the simulation are considered, one with permanent magnets and the other using HTS as a source of excitation. The value of the HTS current is initially determined by means of PM MMF and further iteratively adjusted to obtain a similar radial air gap magnetic flux density as the permanent magnets.

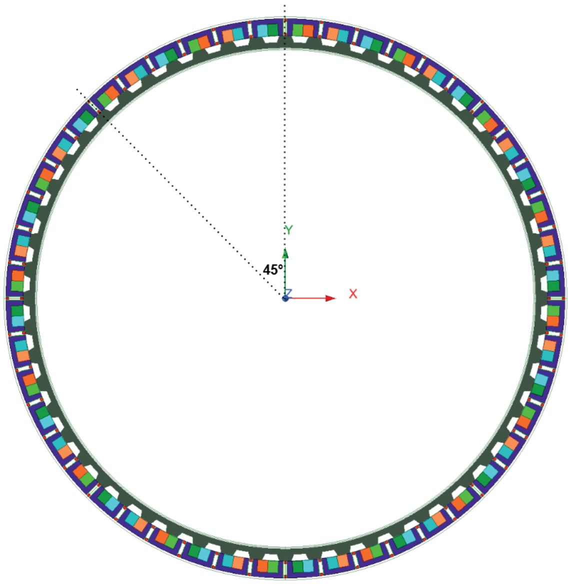

Fig. 7. Full geometry of the model of 48/56 slot/pole FSM [2]

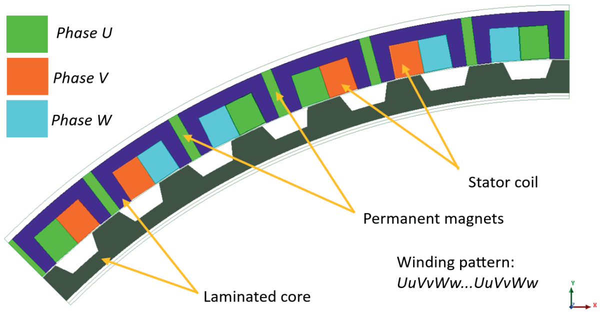

Fig. 8. Reduced geometry due to symmetry conditions (PMs are replaced with HTS coils for HTS excited machine variant)

Table 1. Electrical and mechanical parameters of the machine [2]

Parameter	Symbol	Value
PM remanence flux density (PM variant)	B_r	1.3 T
PM width	w_{pm}	35 mm
Stator outer radius	R_{So}	2660 mm
Stator inner radios	R_{Si}	2500 mm
Rotor outer radius	R_{ro}	2495 mm
Rotor poles	N_r	56
Stator poles	N_s	48
Stack length	l_a	1900 mm
Number of Turns per coil	N	22
Nominal phase current	I_a	456 A
Hts current (Hts variant)	I_{hts}	40.5 kA

Results

The numerical and analytical calculation were carried out at a position of the rotor which is illustrated in Fig. (8). First the current was set to zero to get the field density contribution from the permanent magnets. Then the permanent magnets were treated as air and a current of $(\sqrt{2}\,I_{eff}, -\frac{I_{eff}}{\sqrt{2}}, -\frac{I_{eff}}{\sqrt{2}})$ were fed into the coil.

The following assumptions were made to simplify the problem:

- No saturation is considered, therefore the iron permeability is assumed to be infinite.
- The rotor tooth is assumed to be rectangular with a slot opening equal to the average outer and inner slot openings of the trapezoidal rotor tooth.

Permeance functions

Using equation (21) the following diagrams for the permeance function of the Stator, Rotor and PMs were obtained.

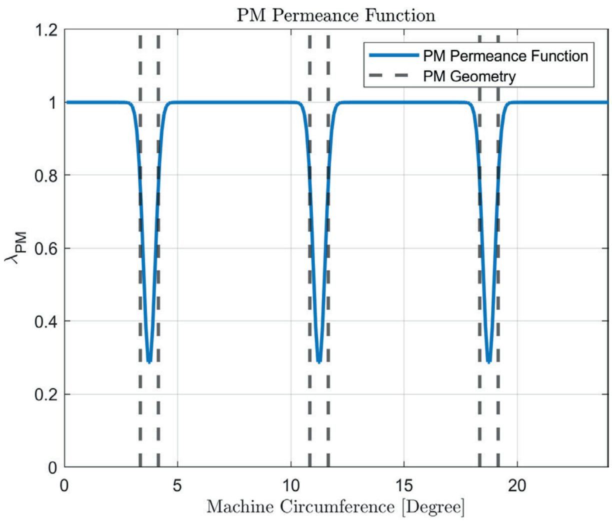

Fig. 9. Permanent magnets permeance function

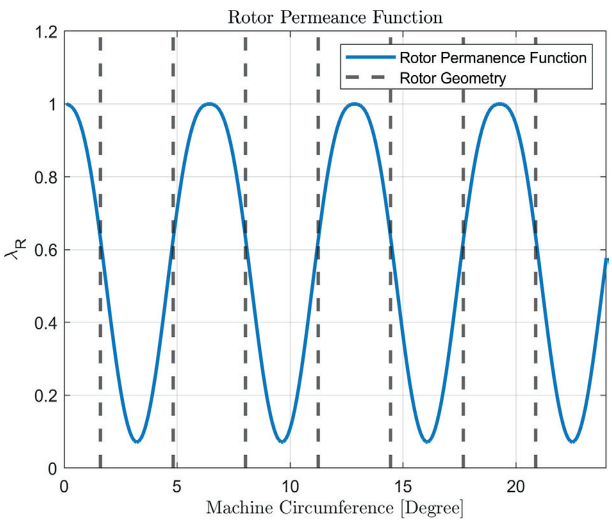

Fig. 10. Rotor permeance function

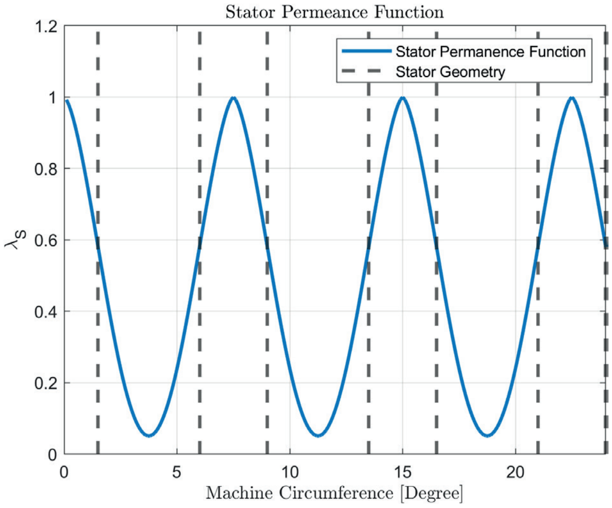

Fig. 11. Stator permeance function

Permanent magnet/HTS flux density

Using equations (3), (4), (7) and (22) the following results are obtained for the permanent magnet/HTS flux density in the air gap.

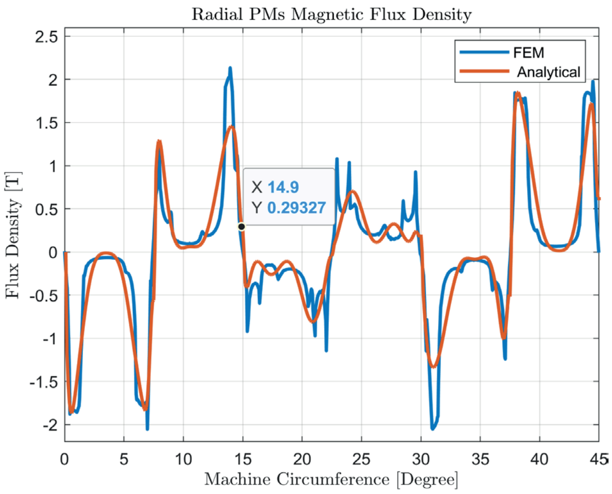

Fig. 12. Air gap radial flux density permanent magnets – *No load*

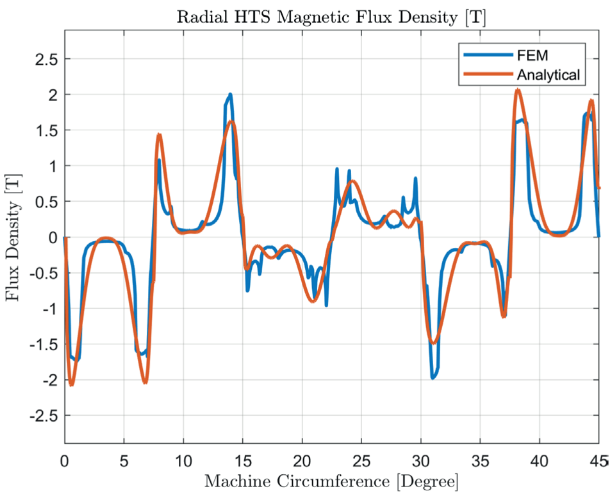

Fig. 13. Air gap radial flux density for HTS winding – *No load*

Stator flux density

For the armature reaction flux density four cases of supplied effective current (50A, 100A, 350A, 450A) were considered. Using equations (11-14), (22) and a super position algorithm the following air gap flux densities are obtained.

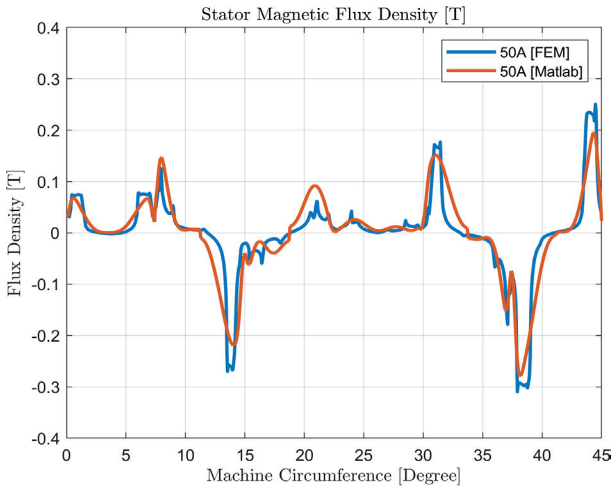

Fig. 14. Air gap radial flux density (50A) – *No permanent magnets*

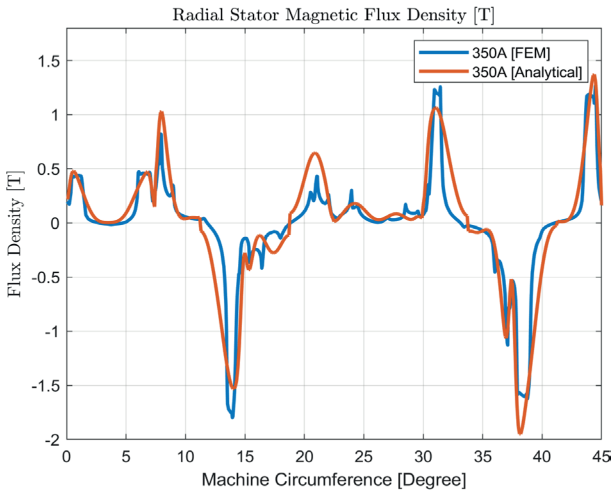

Fig. 15. Air gap radial flux density (350A) – *No permanent magnets*

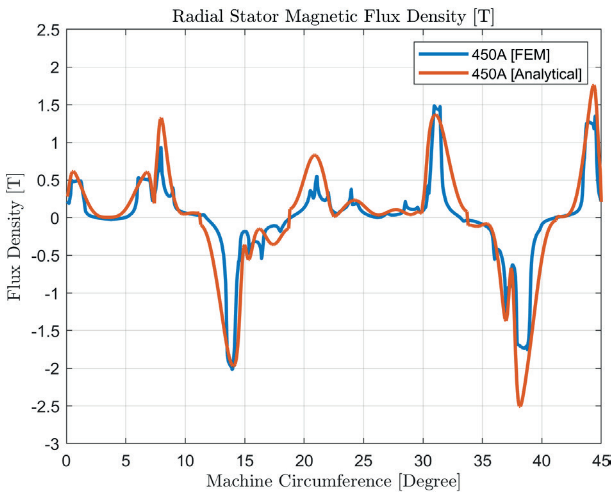

Fig. 16. Air gap radial flux density (450A) – *No permanent magnets*

FEM simulation

While no analytical calculations were made regarding the tangential component of the air gap flux density the following results were obtained from FEA analysis.

Conclusion

The analytical model can make accurate prediction regarding the shape and value of the permanent magnets and stator air gap flux densities. Some spikes could be observed in Fig. 12 as the FEM results are higher than predicted by equation (3), this could be attributed to further flux concentration effect due to influence from the next slot, which could be seen in Fig. 19, this cannot be included without a more detailed MEC of the system that considers the reluctance at every interval [5]. Greater error is observed in the HTS case due to a higher value of flux leakage (Fig. 20.A). The differences could be explained with the magnetization

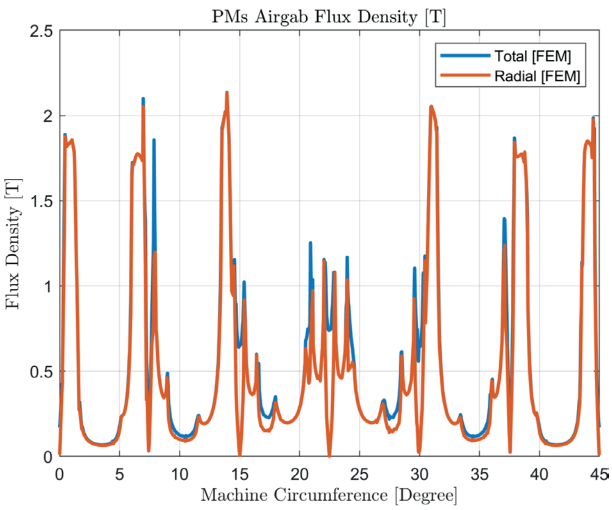

Fig. 17. PMs resultant vs radial component flux density

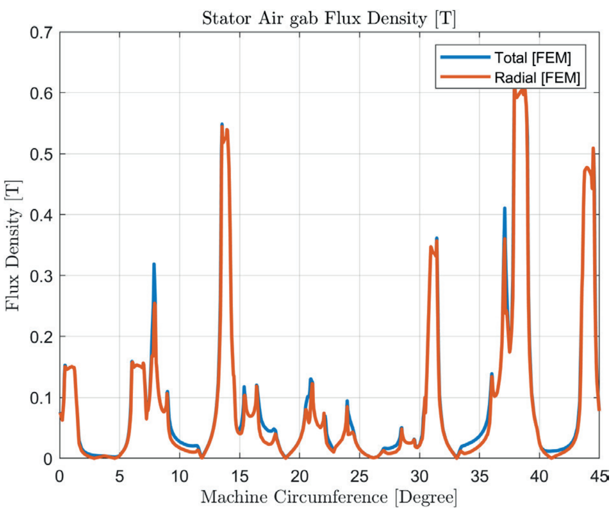

Fig. 18. Stator resultant vs radial component flux density [100A] – *No permanent magnets*

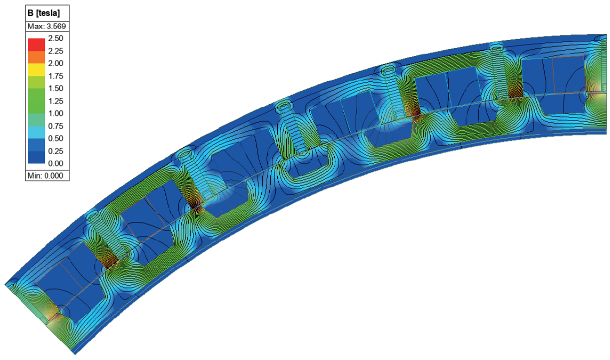

Fig. 19. Magnetic flux density FEM simulation (permanent magnets)

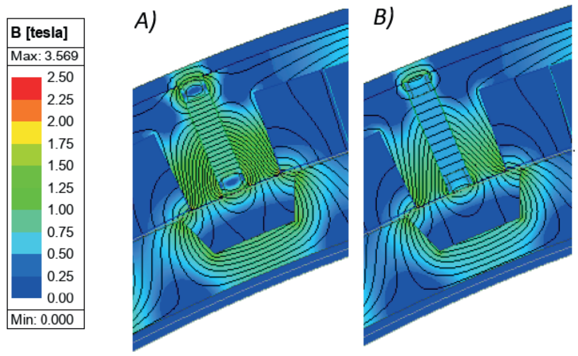

Fig. 20. A) HTS excitation, B) Permanent magnets

method in FEA which is uniform across the magnet surface in the case of permanent magnets. The model accuracy decreases in the range [15° – 30°], which is the case where the rotor and stator teeth do not align (Fig. 8). At this range the tangential component of the air gap flux density of the permanent magnets is biggest (Fig. 17). The tangential component of the stator field could be neglected (Fig. 18). Other error is observed at the peaks (Fig. 14) which is due to flux concentration and rectangular slot assumption at lower currents. The effect of saturation is also visible in sections with high flux density when increasing the current, which drives the analytic calculation higher than the FEA. Since the tangential component of the flux density is not predicted, methods such as the Maxwell stress tensor cannot be directly applied to evaluate electromagnetic or cogging torque. However, using the energy method as in [1] such calculation is possible. Furthermore, neglecting the tangential component, the radial forces could still be calculated. This proves the model valuable during the preliminary design phase of flux-switching machines, where the design space is too broad to rely solely on FEA.

Received: 29.09.2025, **Accepted:** 24.10.2025, **Published:** 24.11.2025

REFERENCES

[1] A. Abdelkefi, A. Souissi and I. Abdhennader, ”Analytical Investigation of Flux Switching PM Machines: Air Gap Flux Density Formulation,” 2022 Second International Conference on Sustainable Mobility Applications, Renewables and Technology (SMART), Cassino, Italy, 2022, pp. 1–7, doi:10.1109/SMART55236.2022.9990436.

[2] M. Lehr, D. Dietz and A. Binder, "Electromagnetic design of a permanent magnet Flux-Switching-Machine as a direct-driven 3 MW wind power generator," 2018 IEEE International Conference on Industrial Technology (ICIT), Lyon, France, 2018, pp. 383-388, doi: 10.1109/ICIT.2018.8352208.

[3] B. Gaussens, E. Hoang, O. de la Barriere, J. Saint-Michel, M. Lecrivain and M. Gapsi, "Analytical Approach for Air-Gap Modeling of Field-Excited Flux-Switching Machine: No-Load Operation," in IEEE Transactions on Magnetics, vol. 48, no. 9, pp. 2505-2517, Sept. 2012, doi: 10.1109/TMAG.2012.2196706.

[4] J. Laksar and L. Veg, ”Numerical calculation of the air gap flux density distribution in rotary electrical machines,” 2016 17th International Conference on Mechatronics - Mechatronika (ME), Prague, Czech Republic, 2016, pp.1–8

[5] Tang, Y.; Paulides, J.J.H.; Lomonova, E.A. Analytical Modeling of Flux-Switching In–Wheel Motor Using Variable Magnetic Equivalent Circuits. ISRN Automot. Eng. 2014, 2014, 1–10, https://doi.org/10.1155/2014/530260.